Fano lineshapes of "Peak-tracking chip" spatial profiles analyzed with correlation analysis for bioarray imaging and refractive index sensing

K. Bougot-Robin*[a], S. Li[b], W. Yue[c], L.Q. Chen[c], X.X. Zhang[c], W.J. Wen[b,d], H. Benisty[e]

[a] Institute for Advanced Study, Hong Kong University of Science and Technology, Clear Water Bay, Kowloon, Hong-Kong, China
[b]Department of Physics, Hong Kong University of Science and Technology, Clear Water Bay, Kowloon, Hong-Kong, China
[c]Advanced Nanofabrication, Imaging and Characterization Core Lab, King Abdullah University of Science and Technology, Thuwal 23955-6900, Kingdom of Saudi Arabia
[d] KAUST-HKUST Micro/Nanofluidic Joint Laboratory, The Hong Kong University of Science and Technology, Clear Water Bay, Kowloon, Hong Kong
[e]Laboratoire Charles Fabry, Institut Optique Graduate School, 2 avenue Fresnel, CNRS, Univ P Sud, 91127 Palaiseau, France

e-mail: phwen@ust.hk

ABSTRACT

The asymmetric Fano resonance lineshapes, resulting from interference between background and a resonant scattering, is archetypal in resonant waveguide grating (RWG) reflectivity. Resonant profile shift resulting from a change of refractive index (from fluid medium or biomolecules at the chip surface) is classically used to perform label-free sensing. Lineshapes are sometimes sampled at discretized "detuning" values to relax instrumental demands, the highest reflectivity element giving a coarse resonance estimate. A finer extraction, needed to increase sensor sensitivity, can be obtained using a correlation approach, correlating the sensed signal to a zero-shifted reference signal. Fabrication process is presented leading to discrete Fano profiles. Our findings are illustrated with resonance profiles from silicon nitride RWGs operated at visible wavelengths. We recently demonstrated that direct imaging multi-assay RWGs sensing may be rendered more reliable using "chirped" RWG chips, by varying a RWG structure parameter. Then, the spatial reflectivity profiles of tracks composed of RWGs units with slowly varying filling factor (thus slowly varying resonance condition) are measured under monochromatic conditions. Extracting the resonance location using spatial Fano profiles allows multiplex refractive index based sensing. Discretization and sensitivity are discussed both through simulation and experiment for different filling factor variation, here $\Delta f=0.0222$ and $\Delta f=0.0089$. This scheme based on a "Peak-tracking chip" demonstrates a new technique for bioarray imaging using a simpler set-up that maintains high performance with cheap lenses, with down to $\Delta n=2\times10^{-5}$ RIU sensitivity for the highest sampling of Fano lineshapes.

Keywords: Resonant waveguide grating – Nanofabrication - Correlation - Fano lineshapes – Refractive index sensing – Bioarray imaging – Spatial tracking

1. INTRODUCTION

Refractive index based sensing is frequently used to sense refractive index medium at a chip surface or biomolecules layer on a chip surface. Detection based on resonant condition allows sensitive detection and has been widely developed exploiting surface plasmon resonance (SPR) [1] or dielectric resonant waveguide gratings (RWGs) [2]. The guided wave coupled at the chip surface interacts with the medium to sense. This results in a change in resonant condition. That change might be measured either through profile (most often spectral or angular) or direct imaging.

Integrated Photonics: Materials, Devices, and Applications II, edited by Jean-Marc Fédéli, Laurent Vivien, Meint K. Smit,
Proc. of SPIE Vol. 8767, 876703 · © 2013 SPIE · CCC code: 0277-786X/13/$18 · doi: 10.1117/12.2018316

2. RESONANT WAVEGUIDE GRATINGS BASED IMAGING

2.1 Resonance waveguide grating sensing

Resonant waveguide gratings have advantages in term of optical configuration (direction of the incident wave) as well as spatial extent of the wave, to optimize coverage with biomolecules. In this paper, we discuss RWGs sensing and exploit Fano profiles from SiN/glass nanostructured chip. Fig. 1 illustrates (A) biolayer sensing and (B) bulk refractive index sensing. In Fig. 1(C), we illustrate spectral Fano profiles with and without biological layer of 4 nm thickness. Similar shift may be observed for an increased of bulk refractive index solution Δn. Profiles are calculated using scattering matrix formalism [3][4]. The immobilization of biomolecules at the chip surface induces an increase of the refractive index, and a shift of the resonant profile. The change of resonance condition might be measured either through the shift directly or in a fixed illumination condition (λ_0, θ_0) as a change in reflectivity ΔR.

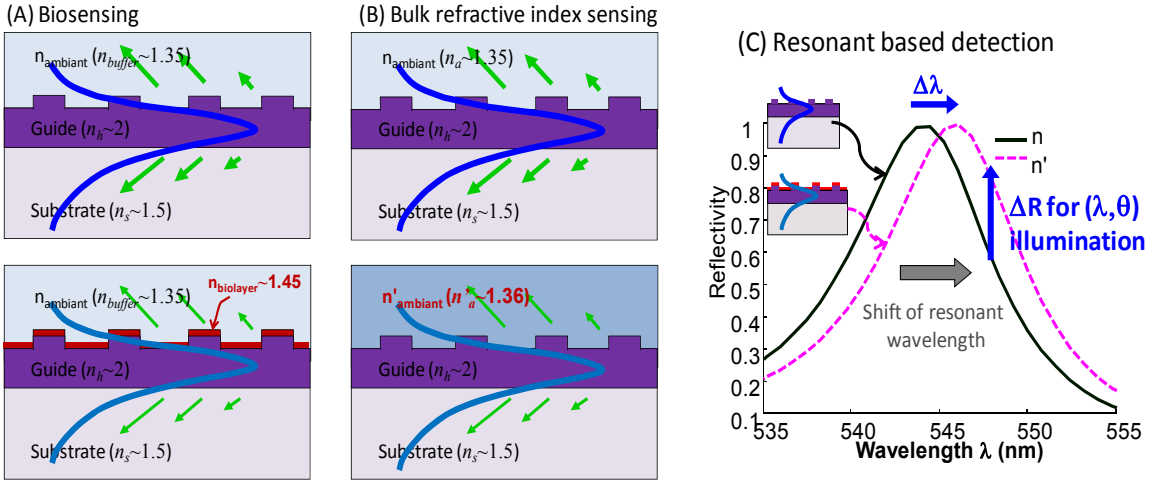

Fig. 1. (A) Resonant waveguide grating chip used for biosensing: the biolayer of index n=1.45 compared to buffer solution n=1.395 and induces a change of guiding properties. (B) Resonant waveguide grating chip used for bulk refractive index sensing. Change of refractive index of the bulk solution induces change of resonant condition (C) Change of resonant condition results in a shift of the spectral response, measured at fixed angle. For a given wavelength, it also results in a change of the intensity value ΔR..

2.2 "Peak-tracking chip" imaging

RWGs direct 2D imaging is advantageous in term of set-up, as no scanning of parameters is necessary. The chip is illuminated in resonant condition (λ_0, θ_0) and a simple picture allows determining the change in reflectivity ΔR, as illustrated in Fig. 1(C). Such configuration has been demonstrated at end point detection on a dried monolayer of biomolecules [5]. Real-time detection brings new issues in term of background and stability. Therefore, an intensity sequence of the Fano lineshape resonance, spectral, angular or spatial, is preferred for robust sensing. Spectral scheme have been developed and commercialized [2, 6]. For spectral based measurement, sensing in a 2D array format is ensured either using a spectro-imager [2] or tunable light source [6]. An alternative is angular scan. However, for sensitive sensing, it requires highly precise mechanical control and has been demonstrated only in research [7]. Scanning an instrumental parameter, either the wavelength or the angle, results in costly instrumentation and larger amount of data. Therefore, there is large interest in robust direct 2D imaging. We recently proposed a scheme combining sequence measurement and simple instrumentation, by varying a parameter in the chip itself rather than in the instrumentation [8].

Our scheme exploits nanostructuration of the chip, to span around the resonance. By smoothly varying a parameter of the grating itself, a spatial Fano profile can be obtained from a simple monochromatic picture. To obtain multiplex detection, several "sensing tracks" can be realized on a same N×P array. In Fig. 2 (A), we give a scheme of our measurement set-up to obtain monochromatic images. For multiplex sensing purpose, several tracks might be imaged in parallel, as illustrated in Fig. 2(B). To span around the resonance, several parameters of the RWGs might be varied (etching thickness, guiding layer thickness, groove width or equivalently filling factor, period). For multiplex sensing and fabrication issues in a 2D geometry, we choose here to vary the filling factor $f_m=d_m/\Lambda_m$. Tracks therefore consists in

a multitude of RWGs micropad units, with filling factor varying by Δf between two adjacent units, as illustrated in Fig. 2 (C).

To sense different bulk media in parallel, a fluidic structure may be designed to have different refractive index media on each of the track. Similarly, for bioarray imaging, different biological species may be immobilized on each of the tracks with adequate chip preparation process.

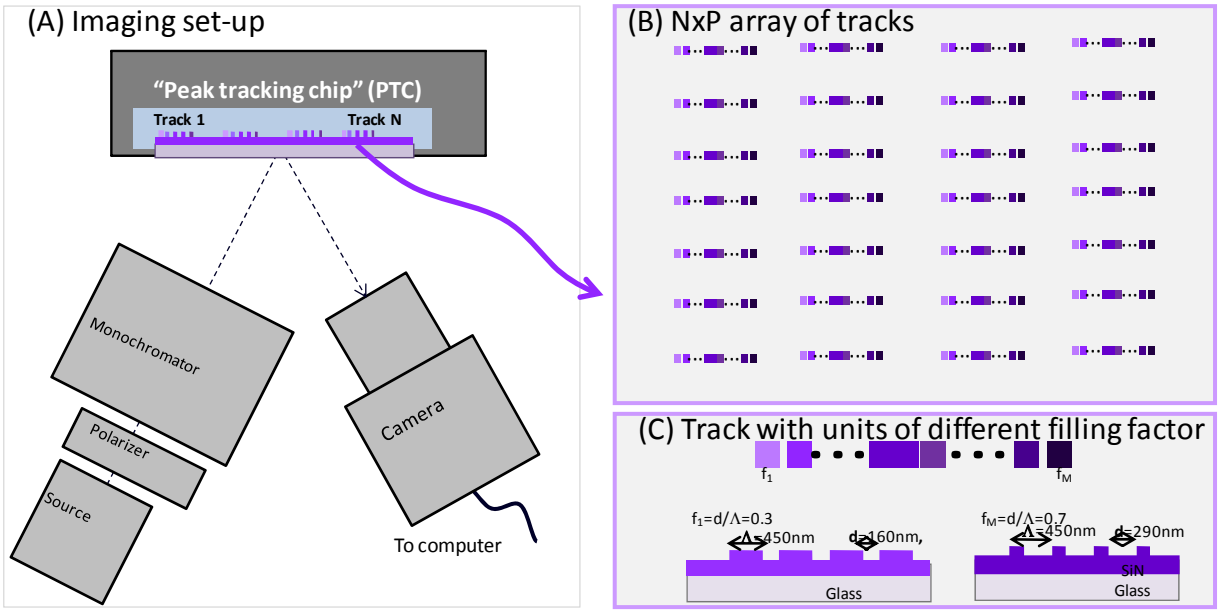

Fig. 2: (A) Imaging set-up: the chip is illuminated with monochromatic and angularly filtered polarized light. The chip image is measured by commercial camera (B) scheme of a N×P array of tracks (C) Details of a track, composed by units of neighboring resonant condition through groove width d_j variation and corresponding filling factor $f_j=d_j/\Lambda$, with Λ the period of the grating.

3. FANO LINESHAPE DISCRETE PROFILES

3.1 Discrete Fano lineshapes

Due to machine and software limitation in the electron beam lithography process, the filling factor is varied discretely, by varying the groove width between each micropad units. For detection in green, we choose a constant period Λ=450 nm for our different micropad units. The groove width variations considered in this paper are of Δd=10 nm and Δd=4 nm respectively..

The chip is illuminated from backside and the reflectivity is simulated for an incident angle of θ=18° with wavelength λ=545 nm._The profiles are calculated considering 2 different bulk refractive index solutions: one of index n=1.35 and the other one of index n=1.36.

Fig. 3 gives the corresponding simulated Fano profiles for a structure composed of silicon nitride waveuiding layer (n=2) on glass substrate (n=1.5),. The SiN layer thickness is of 0.27 Λ, etched on a thickness of 0.1 Λ, where Λ is the grating period, here Λ=450 nm. ,In Fig. 3(A), we give profiles for a continuous variation of the filling factor (it would correspond to continuous variation of the groove width). In Fig. 3 (B) the filling factor variation is of Δf=0.0222, or equivalently a groove width variation of 10 nm with our grating period of Λ=450 nm. In Fig. 3(C) the filling factor variation is of Δf=0.0089, or equivalently a groove width variation of 4 nm with our grating period of Λ=450 nm.

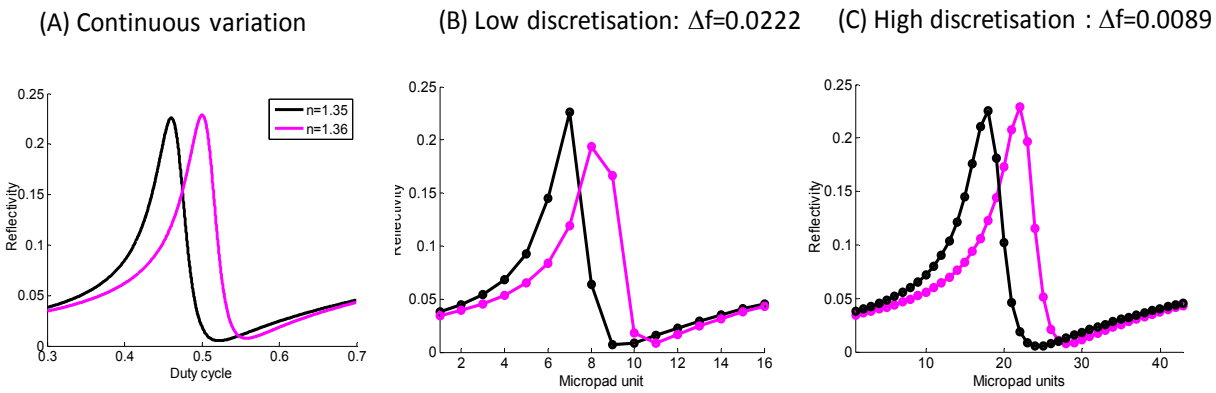

Fig. 3 (A) Spatial profile of the track with sensing media of refractive index n=1.35 and n=1.36, with continuously varying filling factor (B) Discrete profile obtained for a groove width variation of Δd=10 nm, corresponding to a filling factor variation of Δf=0.0222 for a period Λ=450 nm. The refractive index variation per micropad unit is of $\Delta n \sim 10^{-2}$ (C) Discrete profile obtained for a groove width variation of Δd=4nm, corresponding to a filling factor variation of Δf=0.0089 for a period Λ=450 nm. The refractive index variation per micropad unit is of $\Delta n \sim 4\times10^{-3}$.

3.2 Fano profiles using correlation analysis

In a recent study, we compared fitting of discrete Fano profiles with usual fitting models, namely Gauss and Lorentz, and correlation analysis [9]. We demonstrated that correlation analysis was more robust to Fano lineshape asymmetry and gave better accuracy. We remind here how the shift is determined using correlation analysis.

We call S the signal to analyze and S_{ref} the reference signal, which is used to determine the peak shift and then deduce the change of refractive index at the chip surface. Here the signal images consist in 2D matrix, of dimensions $D_x \times M\ D_y$, where M is the number of micropad per track and D_x and D_y are the number of pixels spanning a micropad in both directions. The number of pixels in the vertical direction might D_y=1, and therefore our correlation analysis model can be applied to any Fano lineshapes signal. This shift in micropad unit is considered as proportional to the refractive index change at the chip surface. Note nevertheless that for a large refractive index span, a curvature is observed and a calibration might be necessary to determine the peak shift.

Except from parasitic contributions the D_x lines ideally have the same signal, and we therefore calculate the correlation on each of the lines between the signal and the reference images and average over the different lines. The difference between the lines may have optical origins (for instance distortion) or be due to fabrication variability. Noise contribution is also different on each of the pixel (i, j).
The correlation function can be expressed as follow:

$$C(\Delta j) = D_x^{-1} \Sigma_j \Sigma_i \, \bar{S}(i,j) \otimes \bar{S}_{\mathrm{ref}}(i,j) \tag{1}$$

To increase the precision of this correlation beyond the micropad unit and perform sensitive sensing, meaning have a precise determination of the position of the resonance, we calculate the centroid of the correlation function after correcting it from its average and bringing it at a high power exponent k. This operation serves as limiting tail contribution in our determination.
The corresponding correlation function C' is given by equation (2):

$$C'^{k} = (C - \langle C^2 \rangle)^k \tag{2}$$

In this paper, we use an exponent k=10, both to analyse the simulated resonant response and the experimental profiles. The spatial shift of the track profile may be quantified in micropad unit Δm. Its value may be used to determine an analyte refractive index or a biolayer thickness in the case of biosensing.

$$\Delta m_{sensed} = \sum \Delta m \, C'^{k}(\Delta m) / \sum C'^{k}(\Delta m) \tag{3}$$

3.3 Spatial profiles from "Peak-tracking chip"

Using resonant profiles simulated from our structure parameter, we study the accuracy of correlation analysis for different filling factor variation. Our structure consists in a SiN/Glass resonant waveguide grating, with period Λ=450 nm. The thickness of the SiN layer is of 0.27Λ, and it is etched with a depth h=0.1Λ. The filling factor is varied between f~0.3 and 0.7.

Image profiles are calculated for a bulk refractive index medium from 1.35 to 1.36, and we give in Fig. 4 (A,B) the reflectivity maps for filling factor step respectively of (A) Δf=0.0222 and (B) Δf=0.0089. Each line of the map corresponds to an image profile as we would measure in monochromatic illumination conditions. We apply correlation analysis to these simulated resonant profiles and plot the determined position in red on the reflectivity map.

From our simulation, we can determine the change of resonant peak position in term of micropad for a given change of refractive index Δn. As observed from Fig. 4(A), for a filling factor variation Δf=0.0222, the refractive index change per unit is of $\Delta n=10^{-2}$. From Fig. 4(B), we see that for a filling factor variation of Δf=0.0089, the refractive index variation per micropad unit is $\Delta n=4\times10^{-3}$. Therefore, to obtain a sensitivity $\Delta n\sim10^{-5}$, which is desirable for biosening and sensitive refractive index sensing, fitting of Fano profiles is necessary. This might be realized using correlation analysis as presented in previous section. In Fig. 4(A) and (B), the resonance position as determined by correlation analysis is also given in red on each of the map.

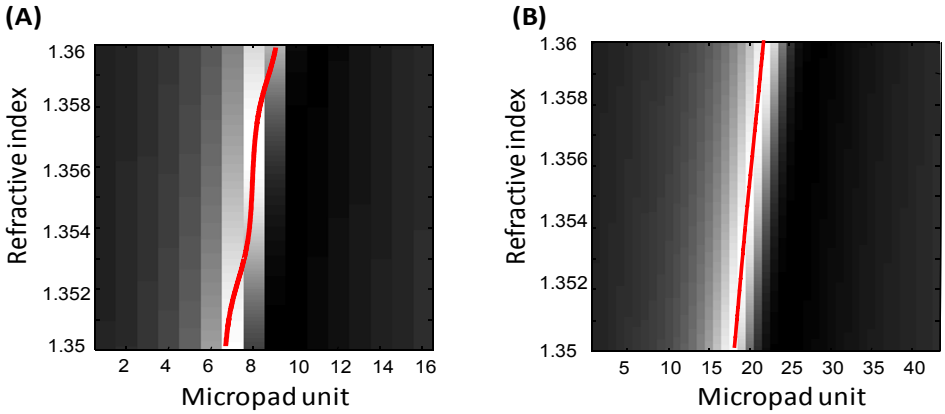

Fig. 4: (A) Reflectivity map obtained for a groove width variation of Δd=10 nm, corresponding to a filling factor variation of Δf=0.0222 for a period Λ=450 nm . The bulk refractive index span is of $\Delta n=10^{-2}$, varying from 1.35 to 1.36. The correlation fit is plotted in red on the graph (C) Same a in (B) for a groove width variation of of Δd=4nm, corresponding to a filling factor variation of Δf=0.0089.

3.4 Discretisation and sensitivity

To determine the sensitivity of our technique, we study the error of the determined peak position to the targeted refractive index value. For the lowest sampling Δf=0.0222, we obtain an error in resonance position determination of $\Delta m=\pm0.15$. This means that the corresponding limit in sensitivity is of $\Delta n=1.5\times10^{-3}$. For the sampling Δf=0.0089, the peak can be determined accurately, and the error in determination will therefore originates from experimental error. With such a scheme, we recently determined that a precision of $\Delta n=2\times10^{-5}$ can be obtained experimentally [9]. Experimental errors may result from noise contribution or different variation such as mechanical vibrations. This means that our new technique for direct 2D RWGs imaging provides sufficient sensitivity for bioarray imaging application as well as refractive index determination down to $\Delta n=2\times10^{-5}$, sufficient for most applications.

4. EXPERIMENTAL RESULTS

4.1 Chip fabrication

The chip consists of borosilicate glass substrate (n~1.47), covered by high-frequency PECVD silicon nitride layer of index n~2.07+0.003i. Nano-structuration is then realized using an electron-beam lithography process [8]. To prevent accumulation of charges from the electron beam on our dielectric chip, we first sputter 5 nm Cr layer on the support in Cooke evaporation system. Photoresist ZEP-7000 is spin-coated at 2000 rpm and backed for 1 min at 180°C prior to exposure. Exposure is realized with a JEOL JBX-6300FS ebeam system using high-precision mode to vary the groove width by step of 4, with a 100 kV energy, 1 nA current and dose 50 mC/cm2). The photoresist is then developed with ZEP500 developer. The uncovered part of chromium is etched away by reactive ion etching process using an AST Cirie 200 machine. The SiN layer is then etched on 50 nm thickness with an AME8110 RIE according to an established process. The remaining photoresist is then stripped by O2 plasma process for 20 min at 100°C temperature in O2 Asher. The remaining chromium is finally etched away using RIE again.

4.2 Refractive index determination

We here present refractive index sensing experiments for refractive index span from 1.333 to 1.475 for the tracks with filling factor by step $\Delta f=0.0089$.

We use a chip array of 2×1 tracks, where one of the track serves as reference (for instance to correct from mechanical instabilities contributions) while on the other track, media with varying refractive index are circulated. To insure maximum stability as well as avoid thermo-optic effect, the media are circulated by using syringe pump with a flow rate of 150 µL/min. We also allow the sample to reach the chamber with enough subsequent time for stabilization. Pictures are taken under an incidence $\lambda=545$ nm, angle $\theta=18^{o}$, and in TM polarization.

To obtain solutions of different refractive index, we use water/glycerol solution with different composition. For large refractive index span, proportion of 100:0, 80:20, 60:40, 40:60, 20:80, 0:100 are chosen, thus corresponding to index varying from 1.333 to 1.475 by step of 0.028. Pictures of the tracks for different media are reported in Fig.5 (A) for filling factor step $\Delta f=0.0089$. For better representation of the signal intensity, we use grey level intensity scale. To determine maximum position, we use correlation analysis. The corresponding resonance peak position are given in Fig. 5(B).

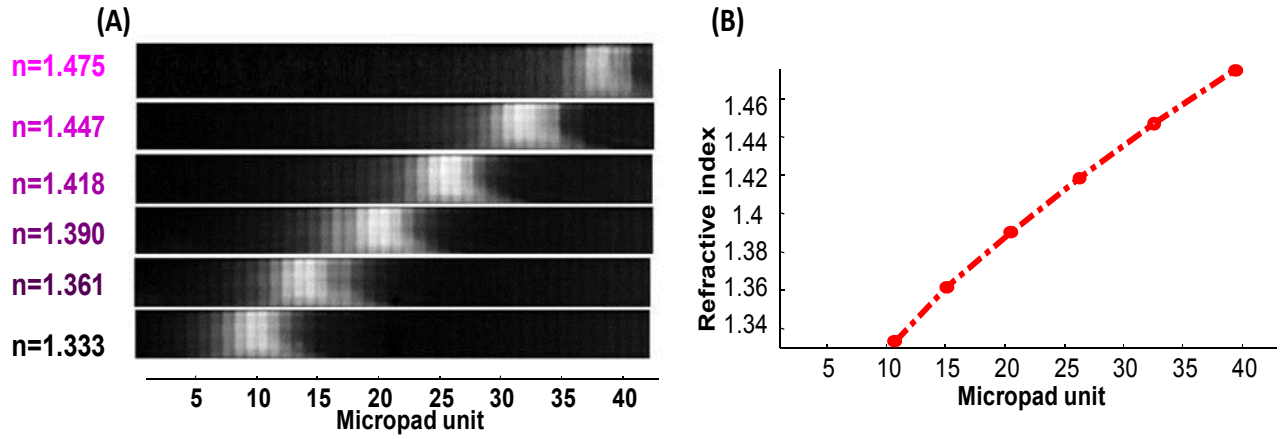

Fig. 5: (A) Track pictures for 6 different water:glycerol solutions, with linearly varying proportion from 0:1 to 1:0 composition, corresponding to a refractive index between 1.333 and 1.475 by step $\Delta n=0.028$ on tracks with filling factor variation between successive micropads $\Delta f=0.0222$ (B) Resonance position from water to glycerol determined by correlation analysis with filling factor variation between successive micropads $\Delta f=0.0222$.

5. CONCLUSION

In this paper, we have presented a new technique for bulk refractive index sensing and bioarray imaging, combining advantages of RWGs based sensing and direct 2D imaging. Robust analysis is allowed by measuring spatial Fano profiles. Integrating the profile dimension inside the chip itself is realised by using a nanostructuration that allows spanning around the resonance peak.

The obtained sensitivity depends on the profile sampling, that latest being imposed by fabrication limitation. We studied two different filling factor cases. A groove width variation of 10 nm (or equivalently a filling factor variation $\Delta f=0.0089$) allows a limit sensitivity of $\Delta n=4\times10^{-3}$. For a groove width variation $\Delta f=4$ nm, the error becomes null in theory.

Experimental results with refractive index span from 1.333 to 1.475 were presented for the chip of filling factor variation $\Delta f=0.0089$. Combining well controlled sample fabrication, stable optic and fluidic set-up as well as robust profile analysis using correlation, a sensitivity down to $\Delta n=2\times10^{-5}$ can been obtained experimentally. This makes our new refractive index sensing platform promising for bioarray imaging [10], to sense biolayer variation in real time with sensitivity down to ~20 pg/mm^2.

ACKOWLEDGMENT

The electron beam lithography project is supported by University Grants SEG_HKUST10. The project is supported by RGC grant 604710 and RPC11SC01.

REFERENCES

[1] Piliarik, M., Homola, J. “Self-referencing SPR imaging for most demanding high-throughput screening applications,” Sensors and Actuators B: Chemical, 134(2), 353-355, (2008).

[2] Li, P.Y. , Lin, B., Gerstenmaier, J. and Cunningham, B. T. “A new method for label-free imaging of biomolecular interactions,” Sens. Act. Chem. 99, 6-13 (2004).

[3] Li, L., “Formulation and comparison of two recursive matrix algorithms for modeling layered diffraction gratings,” J. Opt. Soc. Am. A 13, 1024-1035 (1996).

[4] David, A., Benisty, H. and Weisbuch C. “Fast factorization rule and plane-wave expansion method for two-dimensional photonic crystals with arbitrary hole-shape,” Phys. Rev. B **73**, 075107 (2006).

[5] Bougot-Robin, K., Reverchon, J-L., Fromant, M., Mugherli, L., Plateau, P. and Benisty, H., "2D label-free imaging of resonant grating biochips in ultraviolet," Opt. Express 18, 11472-11482 (2010).

[6] Ferrie, A.M. , Wu, Q. and Fang Y. “Resonant waveguide grating imager for live cell sensing,” Appl. Phys. Lett. 97, 223704 (2010).

[7] George, S. Block, I.D. , Jones, S.I., Mathias, P.C.. Chaudhery, V., Wu, H.Y., Vuttipittayamongkol, P., Vodkin, L. and Cunningham, B.T. “Label-free prehybridization DNA microarray imaging using photonic crystals for quantitative spot quality analysis,” Anal. Chem. 82, 8551-8557 (2010).

[8] Bougot-Robin, K., Li, S., Zhang, Y., Hsing, I.M., Benisty, H., Wen, W. "Peak Tracking Chip for Label-Free Optical Detection of Bio-Molecular Interaction and Bulk Sensing", The Analyst 137(20), 4785- 4794 (2012)

[9] Bougot-Robin, K., Wen W., Benisty, H. "Resonant waveguide sensing made robust by on-chip peak tracking through image correlation", Biomed. Opt. Express 3(10), 2436-3451(2012).

[10] Bougot-Robin, K., Kodzius, R. Yue. W., Chen, L.Q., Li S., Zhang X.X., Benisty H. and Wen W.J. "Real time hybridization studies by RWGs bioarray imaging using nanopattern scanning for Single Nucleotide Polymorphism detection", under review